Biomaterials 161 (2018) 69–80

Contents lists available at ScienceDirect

Biomaterials

journal homepage: www.elsevier.com/locate/biomaterials

High-density lipoprotein-mimicking nanodiscs carrying peptide for enhanced therapeutic angiogenesis in diabetic hindlimb ischemia

Hyun-Ji Park [a, 1], Rui Kuai [b, c, 1], Eun Je Jeon [a], Yoojin Seo [d, e], Youngmee Jung [e, f], James J. Moon [b, c, g], Anna Schwendeman [b, c, **], Seung-Woo Cho [a, h, *]

[a] Department of Biotechnology, Yonsei University, Seoul, 03722, Republic of Korea
[b] Department of Pharmaceutical Sciences, University of Michigan, Ann Arbor, MI 48109, USA
[c] Biointerfaces Institute, University of Michigan, Ann Arbor, MI 48109, USA
[d] NBIT, KU-KIST Graduate School of Converging Science and Technology, Korea University, Seoul, 02841, Republic of Korea
[e] Center for Biomaterials, Biomedical Research Institute, Korea Institute of Science and Technology (KIST), Seoul, 02792, Republic of Korea
[f] Department of Biomedical Engineering, Korea University of Science and Technology (UST), Daejeon, 34113, Republic of Korea
[g] Department of Biomedical Engineering, University of Michigan, Ann Arbor, MI 48109, USA
[h] Center for Nanomedicine, Institute for Basic Science (IBS), Seoul, 03722, Republic of Korea

ARTICLE INFO

Article history:
Received 1 November 2017
Received in revised form
15 January 2018
Accepted 18 January 2018
Available online 19 January 2018

Keywords:
Substance P
High-density lipoprotein
Stem cell mobilization
Diabetic peripheral ischemia
Therapeutic angiogenesis

ABSTRACT

Therapeutic strategies using endogenous stem cell mobilizer can provide effective cell-free therapy for addressing various ischemic diseases. In particular, substance P (SP) exhibited therapeutic regeneration by facilitating mobilization of endogenous stem cells from bone marrow to the injured sites. However, its therapeutic effect has been limited due to short half-life and rapid degradation of administered SP peptides *in vivo*. Here we sought to develop high-density lipoprotein (HDL)-mimicking nanodiscs conjugated with SP (HDL-SP) in order to increase the *in vivo* half-life, bone marrow targeting, and therapeutic efficacy of SP for the treatment of diabetic peripheral ischemia. Conjugation of SP onto HDL nanodisc led to remarkable ~3215- and ~1060-fold increase in the *ex vivo* and *in vivo* half-lives of SP, respectively. Accordingly, HDL-SP nanodiscs improved retention of SP in bone marrow after systemic administration, leading to efficient mobilization of stem cells from bone marrow into blood circulation and reduction of systemic inflammation. Consequently, nanodisc based SP peptide delivery promoted blood vessel formation, blood perfusion recovery and markedly improved limb salvage in diabetic hindlimb ischemia model relative to administration of free SP without nanodisc modification. Therefore, HDL-SP nanodisc can provide a novel strategy for the treatment of diabetic ischemia and HDL nanodisc modification could be potentially useful for the extension of plasma circulation of other labile peptides.

1. Introduction

Stem cell therapeutics, such as mesenchymal stem cells (MSCs) and endothelial progenitor cells (EPCs), have been highlighted as an effective treatment for various ischemic diseases and tissue injuries. Despite advantageous effects of MSCs and EPCs for therapeutic angiogenesis, cell therapies based on exogenously administered cells have encountered several critical limitations, including difficulty in production of a sufficient number of stem cells for transplantation, loss of stem cell phenotypes during long-term *ex vivo* culture, and poor cell survival and engraftment in injured tissues [1]. These limitations have urged emergence of exogenous cell-free approaches by mobilizing endogenous stem cell populations for tissue regeneration and angiogenesis induction [2,3].

Among endogenous stem cell mobilizers, substance P (SP) with 11 peptide sequences has been proposed as an effective endogenous MSC and EPC mobilizer for wound healing and angiogenesis induction. Importantly, Hong et al. identified the new role of SP as an injury-inducible messenger for stem cell mobilization and

* Corresponding author. Department of Biotechnology, College of Life Science and Biotechnology, Yonsei University, 50 Yonsei-ro, Seodaemun-gu, Seoul, 03722, Republic of Korea.
** Corresponding author. Department of Pharmaceutical Sciences, University of Michigan, 2800 Plymouth Rd, Ann Arbor, MI 48109-2800, USA.
E-mail addresses: annaschw@umich.edu (A. Schwendeman), seungwoocho@yonsei.ac.kr (S.-W. Cho).
[1] These authors contributed equally to this work.

https://doi.org/10.1016/j.biomaterials.2018.01.027
0142-9612/

revealed that SP administration accelerated wound healing by facilitating mobilization of $CD29^+$ stromal-like cells from bone marrow to injured tissue [4]. Amadesi et al. also demonstrated that endogenous SP-based nociceptive signaling initiated by injury promoted angiogenesis in critical limb ischemia [5]. The novel function of SP as a stem cell mobilizer could provide highly effective therapeutics for tissue repair without *ex vivo* cell culture and expansion [4–7]. Additionally, SP may be able to induce immune-modulating effects accelerating tissue repair process by suppressing pro-inflammatory factors (*e.g.*, tumor necrosis factor-α; TNF-α) and elevating anti-inflammatory factors (*e.g.*, interleukin-10; IL-10) [4,6–8]. Thus, SP would be an effective therapeutics for the treatment of severe ischemic diseases, including diabetic critical hindlimb ischemia, ulcers, and wounds.

However, therapeutic efficacy of peptide drugs such as SP has been limited by their denaturation and fast degradation by proteases *in vivo* [9]. Thus, the dose and administration frequency of SP peptides should be increased to maintain therapeutically effective dose of SP in blood circulation after systemic administration, which causes substantial side effects and safety issues. Notably, it is known that the diabetic condition increases the level of neutral endopeptidase (NEP), an SP-degrading enzyme, compared with the non-diabetic condition [10]. Indeed, when SP was injected to diabetic mice, the half-life of SP *in vivo* was less than 1 min [11]. Therefore, engineering strategies to increase the *in vivo* stability of SP under diabetic environment should be developed, so that participation of SP in tissue repair process can be prolonged to potentiate the therapeutic efficacy of SP treatment. *In vivo* stability of SP may be improved via SP peptide modification with various chemical and biological moieties as had been shown for other therapeutic peptides [12–15].

In this study, we report a novel SP conjugate, high-density lipoprotein (HDL)-mimicking nanodiscs conjugated with SP, as a highly effective endogenous stem cell mobilizer for the treatment of diabetic peripheral ischemia. HDL, an endogenous nanoparticle involved in the transport and metabolism of cholesterol and lipids, has shown a great potential to extent the circulation time and deliver various cargo molecules, such as proteins, vitamins, hormones, and RNA to various organs [16]. Compared with conventional synthetic nanocarriers, including polymer nanoparticles, liposomes, and inorganic nanoparticles, HDL possesses unique features enabling highly efficient delivery of cargo molecules to target tissues due to its ultra-small size (8–12 nm in diameter), high tolerability *in vivo*, long circulating half-life (12–24 h), and intrinsic targeting capacity to specific tissue types including bone marrow [16–18]. Several studies have demonstrated that HDL-like nanocarriers reconstituted with apolipoprotein (Apo) and Apo-mimetic peptides exhibit similar features as endogenous HDL [16,19–21]. Here, we aimed to exploit the benefits of HDL for delivery of SP. We show that HDL-mimicking nanodiscs incorporated with SP peptide (HDL-SP) significantly prolong the *in vivo* half-life of SP and improve its delivery to bone marrow, thereby augmenting stem cell mobilization and immune modulation for tissue regeneration. We also demonstrate that a systemic administration of HDL-SP nanodiscs can lead to remarkable improvement in therapeutic angiogenesis for the treatment of diabetic peripheral ischemia.

2. Materials and methods

2.1. Preparation of HDL-SP nanodisc formulation

SP peptide with an additional cysteine residue on N-terminus (CRPKPQQFFGLM) and 1,2-dioleoyl-*sn*-glycero-3-phosphoethanolamine-N-[4-(*p*-maleimidophenyl)butylamide] sodium salt (MPB, Avanti Polar Lipids, Alabaster, AL, USA) were mixed at 1.1:1 molar ratio in dimethylformamide (DMF) and allowed to react overnight at room temperature. The reaction mixture was diluted ten times with deionized water and freeze-dried. The obtained lipid-peptide conjugate was then dissolved at 0.3 mM in acetic acid containing 1,2-dimyristoyl-*sn*-glycero-3-phosphocholine (DMPC, Avanti Polar Lipids) and ApoA-1 mimetic peptides (22A, GenScript Corp., Piscataway, NJ, USA) at 2:1 weight ratio, and freeze-dried. The product powder was then hydrated with phosphate buffered saline (PBS, pH 7.4) and cycled 3 times between 50 °C and 4 °C to obtain HDL-SP. The obtained HDL-SP was passed through the desalting column equilibrated with PBS to remove unloaded cysteine-SP peptide. The HDL-SP formulation was lyophilized into powder form for the storage. The powder was reconstituted into solubilized HDL-SP with deionized water right before use. Blank HDL nanodiscs were prepared in the same way as mentioned above without adding the MPB-SP conjugation. LIPO-SP formulation was prepared by dissolving the same amount of DMPC and MPB-SP conjugate in 0.3 mM of acetic acid, followed by freeze-drying. The obtained powder was then hydrated in deionized water and homogenized with a probe sonicator.

2.2. Characterization of HDL-SP nanodiscs

The difference in molecular weight between HDL and HDL-SP nanodiscs was characterized by Gel permeation chromatography (GPC) analysis. Fresh formulation of HDL and HDL-SP samples and their lyophilized and re-dissolved formulation (in PBS) were prepared. HDL and HDL-SP nanodiscs (20 μL) containing 0.5 mg mL^{-1} of 22A peptides were injected into the High-pressure liquid chromatography (HPLC) system equipped with a TSK 2000 GPC column (Sigma-Aldrich, St. Louis, Mo, USA). The flow rate was set at 0.7 mL min^{-1} and the ultraviolet (UV) absorbance of the eluate was measured at 220 nm.

Conjugation between MPB and SP was confirmed by HPLC analysis. Briefly, HDL-SP was dissolved in pure methanol. The prepared HDL-SP nanodiscs, MPB, DMPC, and 22A were filtered through 0.22 μm polytetrafluoroethylene (PTFE) filters before HPLC analyses. Then, the prepared samples were injected into HPLC equipped with a Vydac 219TP diphenyl column (4.6 mm × 250 mm ID, Fisher Scientific, Pittsburgh, PA, USA). Samples were eluted under a binary solvent system consisting of (A) 0.5% trifluoroacetic acid (TFA) in distilled water and (B) 0.05% TFA in the mixture of methanol and acetonitrile (1:1 v/v). The percent of (B) was linearly increased from 15% (0 min) to 100% for 75 min. The system flow rate was set at 0.4 mL min^{-1}. The UV absorbance of the eluate was measured at 220 nm. To confirm the conjugation of cysteine-SP to MPB, the freeze-dried reaction mixture was analyzed using electrospray ionization-mass spectrometry (ESI-MS) with a negative ion detection mode.

To analyze the particle size, dynamic laser scattering (DLS) analysis was conducted. Briefly, 50 μL of HDL or HDL-SP nanodiscs was diluted with 1 mL PBS (pH 7.4) before the measurement on the Malvern Zetasizer Nano ZSP (Malvern Instruments, Malvern, UK). The solution viscosity and refractive index were assumed equal to those of pure water at 25 °C. The effective particle diameters of HDL and HDL-SP nanodiscs were obtained by autocorrelation function using the normal resolution model of the Zetasizer software.

The morphology of HDL or HDL-SP nanodiscs was visualized by transmission electron microscopic analysis (TEM). Sample solution was deposited on carbon film-coated 400 mesh copper grids (Electron Microscopy Sciences, Hatfield, PA, USA) and dried for 1 min. The samples were then negatively-stained with uranyl formate solution, and excessive solutions on the grid were blotted and the grid was dried before TEM observation. All images were acquired on a 100 kV FEI Morgagni TEM microscope (FEI company,

Eindhoven, The Netherlands) equipped with a Gatan Orius CCD camera (Gatan, Inc., Pleasanton, CA, USA).

2.3. Measurement of the half-life of HDL-SP nanodiscs

The half-life of SP, LIPO-SP, and HDL-SP was compared both *ex vivo* and *in vivo* conditions. Briefly, 5 nmol of SP, LIPO-SP, and HDL-SP were added into 100 μL of human blood serum (Sigma-Aldrich) or 50 μL of diabetic rat serum, and incubated in a 5% CO_2 humidified chamber from 0 to 72 h at 37 °C ($n = 4$). The experiment using human blood serum was approved by Institutional Review Board (IRB) of Yonsei University (approval number: 7001988-201704-BR-191-01). To detect SP in the inner portion of the formulations, 5 nM aprotinin (Sigma-Aldrich) was added to each blood serum sample to inactivate NEP activity, and then 0.05% Triton X-100 (Sigma-Aldrich) was added to each sample and incubated at room temperature for 15 min to destabilize the lipid-based formulations. The remaining amount of SP was quantified by Substance P Parameter Assay kit (R&D Systems, Minneapolis, MN, USA).

The SP, LIPO-SP, and HDL-SP degradation kinetics were also analyzed in diabetic mice *in vivo*. Briefly, 2 μg of SP, LIPO-SP, and HDL-SP in 100 μL saline were systemically administrated to diabetic mice via tail vein (ICR mice, female, 6 weeks, Orient Bio, Seongnam, Korea), and blood serum samples were collected at several time points after intravenous injection. The remaining amount of SP was determined by Substance P Parameter Assay kit.

2.4. In vivo biodistribution of HDL nanodiscs

To investigate biodistribution of HDL nanodiscs after systemic administration, HDL nanodiscs were labeled with DiR fluorophore before injection. DiR fluorophores were loaded into the HDL nanodiscs during synthesis. Then, 40 μg of HDL-DiR in 200 μL saline was intravenously administered to Balb/c mice (female, 8–10 weeks, Envigo RMS, Inc., Indianapolis, IN, USA). One day after administration, mice were euthanized and major organs such as brain, heart, liver, spleen, lung, kidney, femur, and tibia were harvested. The fluorescence intensities of HDL-DiR and LIPO-DiR were measured and compared in each organ by using an IVIS Spectrum In Vivo Imaging System (Caliper Life Sciences, Hopkinton, MA, USA).

2.5. Hepatotoxicity evaluation of HDL-SP nanodiscs

Hepatotoxicity of unmodified SP and HDL-modified SP was examined using blood tests that quantified the level of aspartate aminotransferase (AST), alanine transaminase (ALT), and bilirubin in blood serum from ICR mice (female, 6 weeks, Orient Bio, Seongnam, Korea). Briefly, 2.5 nmol kg^{-1} of HDL, and HDL-SP in 100 μL saline was intravenously administered into the mice. PBS injection served as a control. Serum levels of AST, ALT, and bilirubin before injection and 12 and 36 h after intravenous injection were determined using DRICHEM 4000i (Fujifilm, Tokyo, Japan) according to the manufacturer's instructions.

2.6. Injection treatment in a diabetic mouse model with hindlimb ischemia

All animal surgery protocols were reviewed and approved by the Institutional Animal Care and Use Committee of Yonsei University (approval number: IACUC-201607-316-01). Type I diabetes was induced in ICR mice (female, 4 weeks, Orient Bio, Seongnam, Korea) by two-day continuous intraperitoneal injection of 10 mg kg^{-1} streptozotocin (Sigma-Aldrich). Two weeks after diabetes induction, mice with blood-glucose level >400 mg dL^{-1} were selected for hindlimb ischemia induction. To induce hindlimb ischemia, proximal and distal sites of femoral artery of left hindlimb were ligated with a 6-0 prolene suture (Ethicon, Somerville, NJ, USA) and removed surgically. Then, 2.5 nmol kg^{-1} of SP, HDL, LIPO-SP, and HDL-SP in 100 μL saline were intravenously administered via tail vein immediately and 6 days after ischemic injury ($n = 7–14$ for each group). PBS injection served as a control ($n = 13$). The blood flow of ischemic limb was monitored using a laser Doppler perfusion system (Moor Instruments, Devon, UK) on days 0, 2, 7, 14, 21, and 28 after surgery. Blood flow from knee joint to the toe region was analyzed and the blood reperfusion was expressed by calculating the blood perfusion ratio of ischemic limb to normal limb ($n = 6$). According to the criteria for scoring employed in our previous studies [22,23], the severity of the ischemia was categorized as limb loss, foot necrosis, or limb salvage, indicating necrosis or loss above the knee, necrosis below the knee, and normal status, respectively.

2.7. FACS analysis of stem cell mobilization

To quantify mobilized MSC population in peripheral blood mononuclear cells (PBMCs) by HDL, SP, LIPO-SP, and HDL-SP administration, 2×10^7 PBMCs were isolated from peripheral blood extracted from treated mice with diabetic hindlimb ischemia and then incubated with FITC-conjugated anti-CD29 antibodies, allophycocyanin-conjugated anti-CD105 antibodies, and PE-conjugated anti-CD45 antibodies (Miltenyi, Bergisch Gladbach, Germany). To quantify mobilized EPC population of PBMCs, 2×10^7 PBMCs were incubated with FITC-conjugated anti-CD31 antibodies, allophycocyanin-conjugated anti-CD309 antibodies (Miltenyi), and PE-conjugated anti-CD133 antibodies (BioLegend Inc., San Diego, CA, USA). The MSC and EPC fractions in total PBMCs incubated with antibodies were quantitatively analyzed using a FACSCalibur Flow Cytometer (BD Biosciences, Singapore) and the CellQuest software (BD Bioscience).

2.8. ELISA analysis of pro- and anti-inflammatory cytokine release in diabetic hindlimb ischemia

To measure the concentrations of pro-inflammatory (TNF-α) and anti-inflammatory cytokine (IL-10) in serum samples extracted from treated mice with diabetic hindlimb ischemia, ELISA analyses were performed. Briefly, 2.5 nmol kg^{-1} of SP, HDL, and HDL-SP dissolved in 100 μL saline was introduced to mice with diabetic hindlimb ischemia via tail vein injection. Three days after injection, blood was collected via retro-orbital route and serum was isolated to perform ELISA using mouse TNF-α and mouse IL-10 ELISA kits (R&D Systems, Minneapolis, MN, USA). The optical density was measured with the wavelength correction set to 540 nm or 570 nm using an EMax Endpoint ELISA Microplate Reader (Molecular Devices, Sunnyvale, CA, USA).

2.9. Histological and immunohistochemical analyses of the ischemic limb muscle

After 28 days of injection treatments, the mice were sacrificed and ischemic muscles were harvested. The tissue samples were fixed with 10% (v/v) neutral formalin and processed with a TP1020 tissue processor (Leica Biosystems, Wetzlar, Germany) to prepare tissue-embedded paraffin blocks. The tissue sections (4.5 μm in thickness) were prepared and stained with Harris hematoxylin (Sigma-Aldrich) & eosin Y (Samchun Chemical, Pyungtaek, Korea) (H&E) and Masson's trichrome (Sigma-Aldrich).

Immunohistochemical staining of ischemic muscles was

performed as follows: fixed samples were permeabilized with 0.1% (v/v) Triton X-100 in PBS for 15 min, blocked with 4% normal goat serum for 1 h, incubated with primary antibodies overnight at 4 °C, and then sequentially incubated with secondary antibodies for 2 h at room temperature. Capillaries and arterioles in 28-day muscle samples were stained with primary antibodies for anti-CD31 (1:50, Abcam, Irvine, CA, USA) and anti-smooth muscle α-actin (SMA) (1:50, Abcam), respectively, and visualized by Alexa Fluor 488 goat anti-mouse IgG and Alexa Fluor 594-donkey anti-rabbit secondary antibodies (1:200, Invitrogen), respectively. For macrophage staining in 5-day muscle sample, anti-F4/80 (1:100, Abcam) and anti-CD163 (1:200, Abcam) were used and visualized by Alexa Fluor 488 goat anti-rat IgG and Alexa Fluor 594 donkey anti-rabbit IgG antibodies (1:200, Invitrogen), respectively. Nuclei were counterstained with 4,6-diamidino-2-phenylindole (DAPI, Sigma) and examined using confocal microscopy (LSM 880, Carl Zeiss, Jena, Germany).

2.10. Spleen enlargement analysis

Five days after SP, HDL, and HDL-SP treatments to mice with diabetic hindlimb ischemia, spleens were collected from each treated mouse and the weight of the spleens was measured ($n = 4$). After weight measurement, spleens were fixed with 10% (v/v) neutral formalin, processed with a TP1020 tissue processor, sectioned, and stained with H&E. The white pulp area was quantified by using Image J 1.49v software (National Institute of Health, Bethesda, MD, USA).

2.11. Statistical analysis

Data are presented as the mean ± the standard deviation. All the statistical analyses were performed using GraphPad Prism (Graphpad Software, San Diego, CA, USA). Two-way of analysis of variance (ANOVA) and repeated measures of ANOVA were used to determine statistical significance. The p values < 0.01 and 0.05 were considered statistically significant.

3. Results and discussion

3.1. Preparation of HDL-SP nanodisc formulation

In this study, HDL-mimicking nanodiscs for SP delivery were synthesized with Apo-mimetic peptides and lipids. HDL-mimicking nanodisc formulation of SP is expected to protect SP from serum protease and NEP, and increase *in vivo* half-life, ultimately improving the efficiency of SP delivery to bone marrow and its therapeutic efficacy. N-terminus-cysteinyl SP (SP-C) was conjugated with MPB via stable and irreversible thioether linkage (Fig. 1A). It is known that C-terminal residues of SP is critical for its therapeutic efficacy because C-terminal pentapeptide sequence of FFGLM in SP, a characteristic of tachykinin neuropeptides, is involved in SP binding specific to neurokinin 1 receptor (NK1R) [24]. Valentin-Hansen et al. have also shown that C-terminus of SP binds more tightly to the binding site of NK1R than its N-terminus [25]. Thus, MPB was conjugated to N-terminal region of SP to avoid interruption of binding affinity of SP to its receptor. Finally, the resulting MPB-SP conjugate was added to the mixture of DMPC and 22A (Fig. 1B), resulting in the formation of disc-shaped HDL-SP nanoparticles with the average size of 10.3 ± 0.8 nm (Fig. 1C, E). The average thickness of HDL-SP nanodiscs was approximately 2–4 nm, as confirmed by TEM image clearly showing discoidal structures of HDL-SP nanodiscs (Supplementary Fig. S1). In this TEM image, HDL-SP nanodiscs were shown as round shape from the top and disc shape on the side. Our result is similar to that from a previous study reporting that complexation of lipids and ApoA-I mimetic peptides has formulated the nanodiscs [26]. HPLC and mass spectrometry analyses confirmed the conjugation of SP peptides to MPB lipids (Fig. 1D and Supplementary Fig. S2). HDL-SP sample showed the peaks specific to 22A peptide and DMPC at 54–57 min and 71 min, respectively (Fig. 1D), indicating successful incorporation of 22A peptide and DMPC into HDL-SP nanodisc formulation.

Since the length of SP-C is approximately 1.6 nm and the gap between MPB-SP molecules is estimated to be 3–5 nm, the binding of SP to NK1R may not be interrupted. In a previous literature suggesting the structural binding model of SP to NK1R, TEM imaging analysis revealed that the size of NK1R multimers was 3.8 nm [27]. Accordingly, the scale of SP peptide binding with NK1R is expected to be around 4–8 nm. Thus, the gap of 3–5 nm between MPB-SP molecules may not influence the interaction between SP and NK1R. Although the interaction between HDL-SP and NK1R may not be affected by HDL modification, interaction between HDL-SP and neutral endopeptidase can be attenuated by HDL modification. We may find the rationale on this phenomenon from inherent features of HDL particles. It has been known that HDL is associated with many proteins (*e.g.*, growth factors, hormones, and receptors) and protects the associated proteins from degrading enzymes including peptidases and proteinases during circulation [28,29]. Due to this stealth function of HDL from enzymatic degradation, HDL modification of SP may be able to protect SP from endopeptidases while not affecting interaction between SP and NK1R. GPC analysis of fresh HDL-SP samples (Fig. 1F) and rehydrated samples of lyophilized HDL-SP nanodiscs (Fig. 1G) showed no significant difference in retention time, indicating that lyophilization and rehydration of HDL-SP nanodiscs did not affect the size and homogeneity of nanoparticle populations (Fig. 1F and G).

3.2. Increased in vivo half-life and bone marrow retention of HDL-SP nanodiscs

Systemic delivery of peptide drugs has shown limited therapeutic efficacy due to short *in vivo* half-life caused by rapid proteolysis [30]. In HDL-SP nanodisc formulation, HDL could protect the SP peptides from recognition and digestion by proteolytic enzymes, thus, improving the availability of peptides to achieve therapeutic efficacy [12]. The HDL nanodisc system dramatically increased the stability of SP *ex vivo* and its circulation half-life *in vivo* (Fig. 2). In exposure to human normal serum *ex vivo*, HDL-SP nanodisc formulation extended the half-life of SP up to 117 h (3200-fold increase compared with 2.2 min for unmodified SP) (Fig. 2A). When incubated with diabetic rat serum *ex vivo*, HDL-SP exhibited significantly improved SP stability with a half-life of 30 h, whereas free SP showed a half-life of only 1.7 min (Fig. 2B). We also compared the half-life of SP and HDL-SP *in vivo* after intravenous administration into diabetic mice (Fig. 2C). The enzyme-linked immunosorbent assay (ELISA) performed on serum samples isolated from injected mice showed that the half-lives of systemically administered SP and HDL-SP were about 0.8 min and 60 h, respectively (Fig. 2C). In diabetic mice, SP and HDL-SP fully degraded in 5 min and 96 h, respectively (Fig. 2C). Although chemical modification can usually prolong half-life of peptide drugs *in vivo*, extended exposure of peptides to serum components and enzymatic degradation during blood circulation decreases the stability of modified peptides. Thus, in our study, HDL-SP formulation can resist against enzymatic degradation up to certain period of time after intravenous administration (~60 h), but ultimately HDL-SP is destabilized and disassembled over time by increased interaction with serum proteins and enzymatic degradation, leading to accelerated degradation of HDL-SP formulation. Several previous studies have shown sigmoidal degradation profiles of the

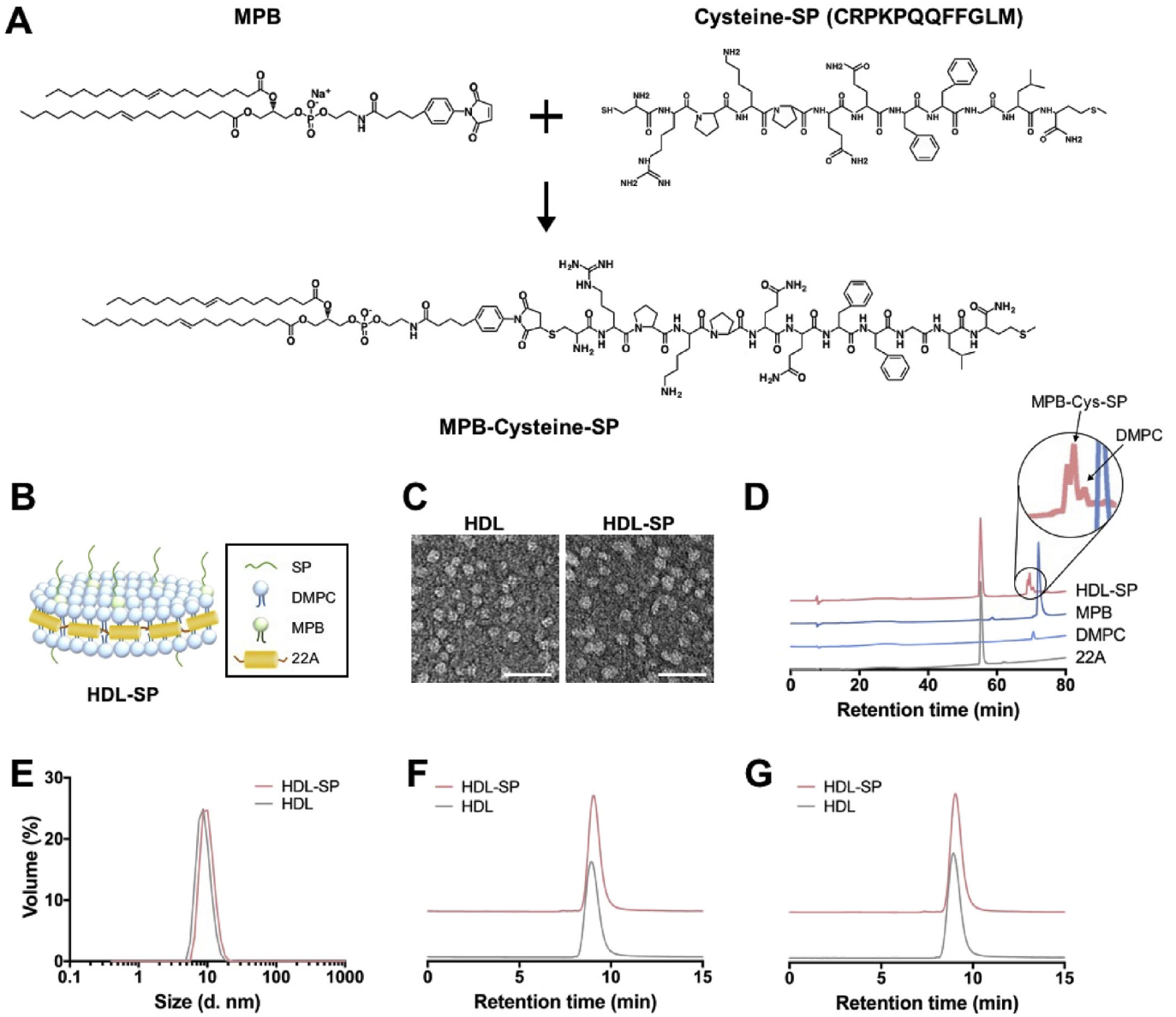

Fig. 1. Synthesis of HDL-SP nanodiscs. (A) Covalent conjugation of MBP to cysteine-SP via thiol-maleimide click reaction. (B) Schematic illustration of HDL-SP nanodisc formulation. (C) Transmission electron microscopy (TEM) images of blank HDL nanodiscs (left) and HDL-SP nanodiscs (right). Scale bars indicate 50 nm. (D) High pressure liquid chromatography (HPLC) analysis of HDL-SP nanodiscs. (E) Dynamic light scattering (DLS) analysis to check the size of HDL and HDL-SP nanodiscs. Gel permeation chromatography (GPC) of (F) fresh formulations of HDL and HDL-SP nanodiscs and (G) lyophilized and rehydrated (with endotoxin-free water) formulations of HDL and HDL-SP nanodiscs.

concentration and half-life of modified peptides or proteins *ex vivo* [31,32], which are similar to the data provided in our current study.

Our previous study demonstrated the important role of 22A peptide on the stability and structure of HDL nanodiscs [19]. Indeed, the half-life of liposomal formulation of SP (LIPO-SP) without 22A peptides was decreased under both *ex vivo* and *in vivo* conditions, compared with HDL-SP nanodisc formulation with 22A peptides (Fig. 2A–C). Some SP peptides may be randomly distributed in the inner membrane portions of LIPO-SP formulation, and thus they could be protected from enzymatic degradation. However, owing to the absence of 22A peptide component that is critically important for maintaining the stability and structures of HDL nanodiscs, LIPO-SP formulation is destabilized more quickly than HDL-SP formulation, showing much shorter half-life of SP peptides. Considering that NEP activity is generally higher in diabetic patients than in normal individuals [10], HDL-SP nanodisc formulation would be more critical to extend the half-life and retention of administered SP in diabetic patients, in turn improved therapeutic regenerative efficacy of SP treatment.

The increased *in vivo* half-life and circulating retention of SP by HDL modification could also enhance accumulation of SP in bone marrow, a target organ of SP, thereby promoting interaction with stem or progenitor cell populations resident in bone marrow. One day after systemic administration of fluorescently labeled HDL nanoparticle formulation, biodistribution of the nanoparticles was examined in the major organs. Fluorescent dye (DiR)-loaded HDL nanodiscs (HDL-DiR) showed much stronger fluorescent signal in the liver, lung, and kidney than DiR-loaded liposome (LIPO-DiR) without 22A peptides (Fig. 2D). Importantly, the fluorescent signal from HDL-DiR was readily detected in both femur and tibia one day after intravenous injection, compared with minimal signal from LIPO-DiR (Fig. 2D). Quantification of the fluorescent signal

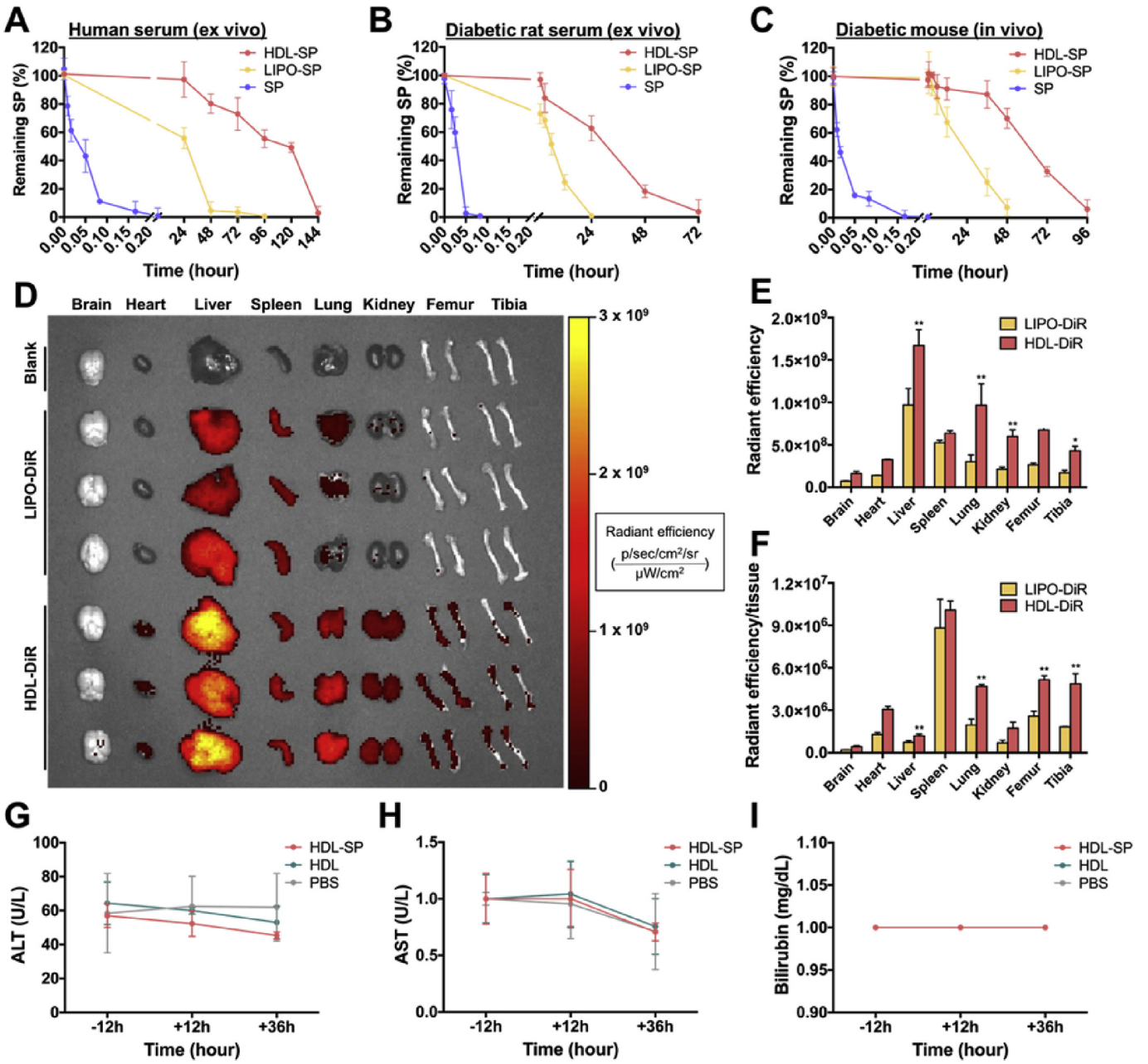

Fig. 2. The pharmacokinetics and toxicity of HDL-SP nanodisc formulation. Half-life of SP, LIPO-SP, and HDL-SP exposed to *ex vivo* condition of ((A) normal human serum and (B) diabetic rat serum. (C) *In vivo* half-life of SP, LIPO-SP, and HDL-SP at several time points after intravenous injection to diabetic mice. (D) Organ distribution of DiR-loaded liposomes (LIPO-DiR) or DiR-loaded HDL nanodiscs (HDL-DiR) 24 h after intravenous administration. Quantification of (E) total fluorescence intensity (p/sec/cm^2/sr/μW/cm^2) in each organ and (F) the fluorescence intensity normalized to tissue weight (p/sec/cm^2/sr/μW/cm^2/mg) in each organ ($n = 3$; $^{**}p < .01$ versus each corresponding LIPO-DiR group). (G-I) Hepatotoxicity evaluation of HDL-SP nanodiscs on the base of the levels of (G) alanine aminotransferase (ALT), (H) aspartate aminotransferase (AST), and (I) bilirubin in serum collected from mice receiving intravenous injection of HDL-SP nanodiscs ($n = 4$).

indicated that the average radiant efficiency for the HDL-DiR group was much greater than that of LIPO-DiR in all organs examined, including femur and tibia (Fig. 2E). Normalization of the average radiant efficiency by tissue weight indicated robust accumulation of HDL-DiR in femur and tibia, whereas most of the fluorescence of LIPO-DiR was observed in the spleen (Fig. 2F). Overall, these results demonstrated significantly increased delivery and retention of HDL nanodiscs to bone marrow, the preferred target organ of SP for stem cell mobilization. Basically, we think that SP accumulation could be enhanced due to prolonged blood circulation by HDL modification in HDL-SP nanodiscs. Additionally, inherent function of HDL in HDL-SP nanodiscs may contribute to enhanced targeting and accumulation of SP into bone marrow. HDL is known to transport lipids and cholesterols through the blood vessels and lymphatic vasculature [33]. Thus, HDL-SP nanodiscs may facilitate SP transport to bone marrow through vasculatures connected to bone marrow. Because several studies have also demonstrated the presence of HDL receptors in several types of bone marrow cells [34,35], HDL-SP nanodiscs may be able to efficiently induce accumulation of SP peptides in bone marrow via HDL receptor-mediated binding.

Importantly, animals treated with HDL-SP nanodiscs did not

exhibit any overt signs of toxicity *in vivo* despite the increased half-life of SP and overall exposure to SP. The levels of AST, ALT and bilirubin in serum isolated from diabetic mice after 12 and 36 h of HDL-SP injection were not significantly changed, compared with the levels in serum measured before injection (Fig. 2G–I). The values of HDL-SP-injected group were not significantly different from those of PBS-injected group at all-time points (before, 12 h, and 36 h after injection) (Fig. 2G–I). These data suggested that systemic administration of HDL-SP formulation was well-tolerated without any overt signs of hepatotoxicity.

3.3. Enhanced stem cell mobilization by HDL-SP nanodiscs in diabetic mice with hindlimb ischemia

HDL-SP nanodiscs significantly enhanced stem cell mobilization from bone marrow to blood circulation even in diabetic conditions known to attenuate stem cell mobilization [36]. Compared with normal animal serum samples, diabetic animals had increased level of NEP activity in serum (Fig. 3A), which may diminish the effect of SP on stem cell mobilization. To understand the impact of SP on mobilization of stem cells, we administered various SP formulations via tail vein into mice with diabetic hindlimb ischemia, and 3 days later, we performed fluorescence-activated cell sorting (FACS) analysis of peripheral blood mononuclear cells (PBMCs) in the blood samples. Intravenous injection of unmodified SP (dose: 2.5 nmol kg^{-1} mouse) did not increase the frequencies of MSC ($CD29^+CD105^+CD145^-$) and EPC ($CD31^+CD133^+CD309^+$) populations in the blood circulation (SP group; 0.06 ± 0.03% of EPC and 0.19 ± 0.06% of MSC, PBS group; 0.04 ± 0.04% of EPC and 0.26 ± 0.20% of MSC, and HDL group; 0.06 ± 0.03% of EPC and 0.17 ± 0.13% of MSC, Fig. 3B and C). Injection of LIPO-SP without 22A peptides also did not increase the level of MSC and EPC populations in the blood circulation (0.02 ± 0.02% of EPC and 0.15 ± 0.08% of MSC, Fig. 3B and C). Importantly, the frequencies of mobilized MSCs and EPCs from bone marrow to blood circulation were dramatically increased by intravenous administration of HDL-SP (dose: 2.5 nmol kg^{-1} mouse) (0.17 ± 0.09% for EPC and 0.69 ± 0.18% for MSC, $p < .01$, Fig. 3B and C). Overall, these results suggested that HDL-SP nanodiscs resistant to proteolysis from NEP in diabetic environment enhanced the circulation half-life and bone marrow-targeting of SP and induced potent stem cell mobilization *in vivo*, thus suggesting their therapeutic potential for angiogenesis and tissue regeneration in diabetic hindlimb ischemia.

3.4. Potentiated immune modulating effects of HDL-SP nanodiscs in mice with diabetic hindlimb ischemia

Immune modulating effect of SP for tissue repair could be potentiated by HDL nanodisc modification in animals with diabetic hindlimb ischemia. As diabetes causes chronic inflammation, finally leading to severe tissue damage, control of inflammation is of great importance in diabetic patients [6,8,37,38]. SP is known to facilitate tissue regeneration by activating the M2 macrophage in the early stage of wound healing and stimulate the secretion of anti-inflammatory cytokines (*e.g.*, IL-10) [39]. After intravenous administration of HDL-SP to diabetic mice with hindlimb ischemia (2.5 nmol kg^{-1} dose), the level of anti-inflammatory (IL-10) or pro-inflammatory cytokine (TNF-α) in blood serum extracted from the injected mice was quantified by ELISA assay 1, 3, and 5 days after injection (Fig. 4A and B). No treatment group with PBS injection showed marginal level of IL-10 and high level of TNF-α in blood serum, but SP injection significantly increased IL-10 level and reduced TNF-α level at early periods of wound healing (Fig. 4A and B). More importantly, when compared with unmodified SP treatment, HDL-SP treatment further increased IL-10 level and decreased TNF-α level in blood circulation (Fig. 4A and B), indicating potentiated immune modulating effects of HDL-SP formulation for the treatment of diabetic ischemia.

In addition, HDL-SP successfully suppressed macrophage infiltration and modulated macrophage polarization for tissue healing in diabetic ischemic tissue. The plasticity of macrophage is known to be of great importance in tissue healing process [40]. The M1 phenotype generating a high level of pro-inflammatory cytokines is associated with sterilizing function that causes strong biocidal activity and tissue damage [40]. In contrast, M2 macrophages are involved in tissue remodeling and immune regulation for tissue healing [40]. Thus, we quantified macrophage infiltration and macrophage polarization (M2/total macrophage ratio) in diabetic ischemic muscle after SP treatment. In a normal condition, the muscle structure was intact and infiltration of inflammatory cells including macrophages was not observed in muscle fibers, while ischemic injury impaired muscle tissue and induced significant infiltration of inflammatory cells into muscle fibers (Fig. 4C and D). Treatment of HDL-SP nanodiscs substantially attenuated macrophage infiltration into the ischemic region, compared with control groups including unmodified SP treatment (Fig. 4D and E). Importantly, HDL-SP activated macrophage polarization favorable for tissue healing process. The relative population of M2/total macrophages ($F4/80^+CD163^+$ cells to $F4/80^+$ cells) was the highest in HDL-SP group among the tested groups (16.5 ± 13.6% in normal group, 7.2 ± 2.8% in PBS group, 40.1 ± 6.1% in HDL group, 29.1 ± 5.4% in SP group, and 56.7 ± 10.8% in HDL-SP group) (Fig. 4F). Almost 60% of the infiltrated macrophages in HDL-SP group were found to exhibit M2 phenotype, indicating that the immune modulation of SP could be enhanced by HDL modification. Surprisingly, administration of HDL nanodiscs without SP also showed an immune

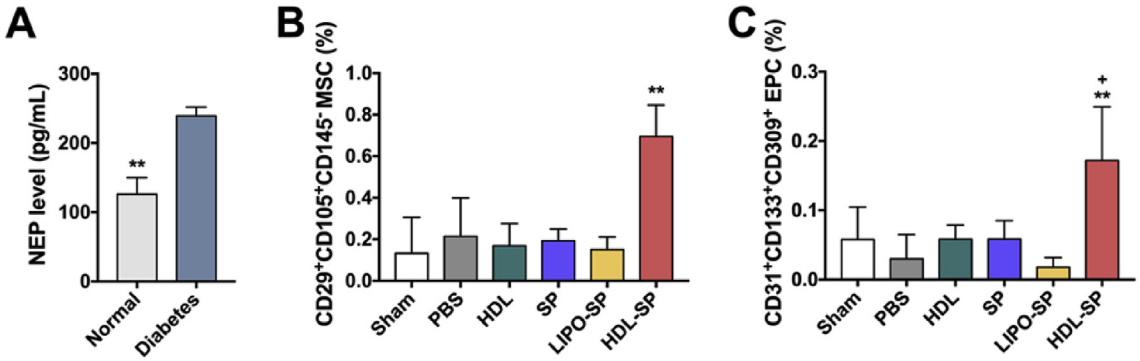

Fig. 3. Mobilization of endogenous stem cell populations in blood circulation 3 days after intravenous HDL-SP administration in diabetic mice with hindlimb ischemia. (A) The serum levels of NEP in normal and diabetic mice ($n = 3$; $^{**}p < .01$). FACS analyses of (B) MSC population ($CD29^+CD105^+CD145^-$) in total PBMCs from diabetic mice ($n = 4$; $^{**}p < .01$ versus other control groups) and (C) EPC population ($CD31^+CD133^+CD309^+$) in total PBMCs from diabetic mice ($n = 4$; $^{**}p < .01$ versus PBS and LIPO-SP groups, $+p < .05$ versus sham, HDL, and SP groups).

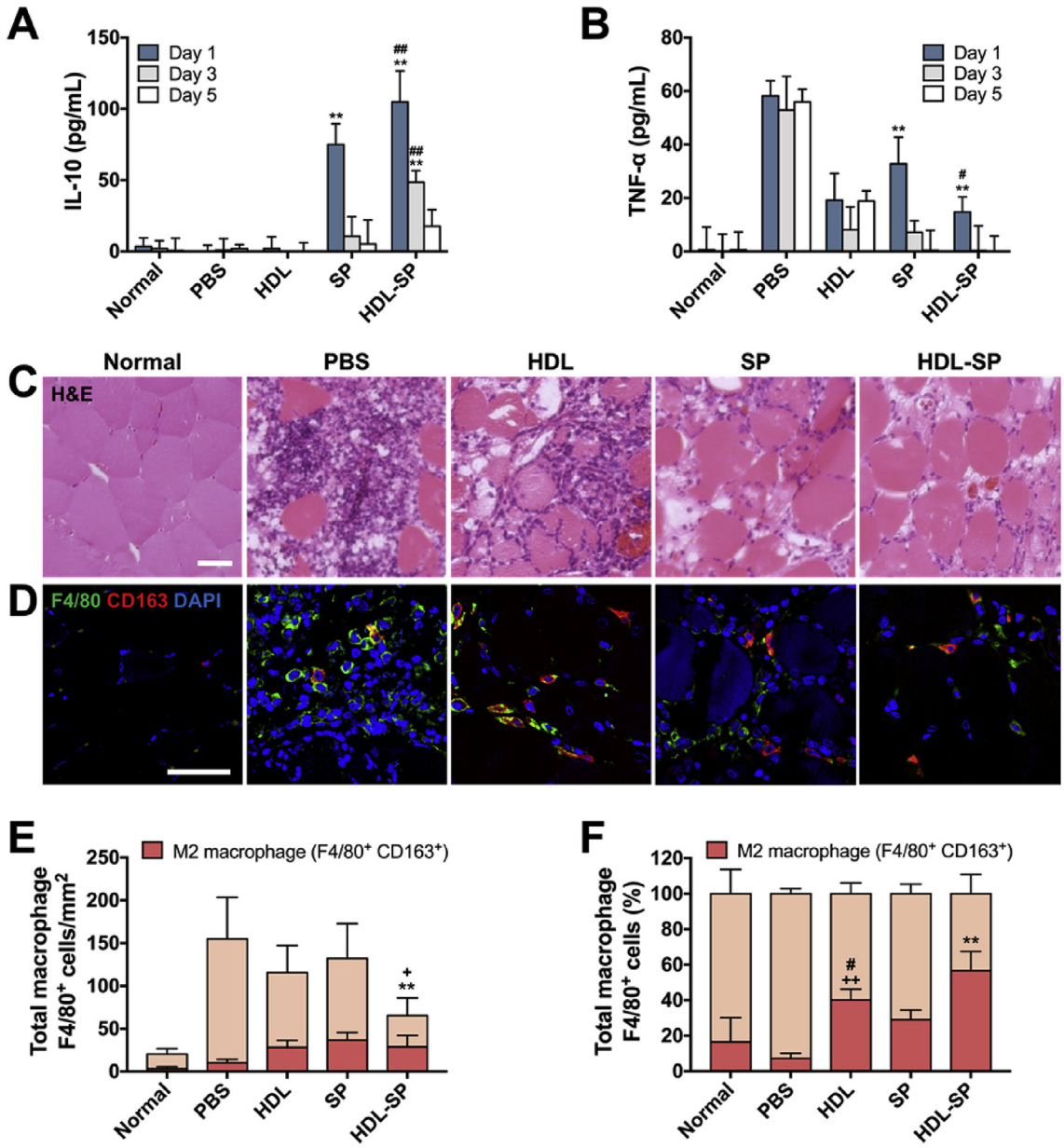

Fig. 4. Enhanced immune modulating effects of HDL-SP administration in diabetic mice with hindlimb ischemia. The serum levels of (A) anti-inflammatory cytokine IL-10 and (B) pro-inflammatory cytokine TNF-α in each group measured by ELISA analysis ($n = 3–4$; $^{**}p < .01$ versus normal, PBS, and HDL groups at the same day, $\#p < .05$ and $\#\#p < .01$ versus SP group at the same day). (C) H&E staining of diabetic hindlimb muscles 5 days after ischemic injury development and injection treatments. Scale bar indicates 100 μm. (D) Immunofluorescent staining F4/80 (green) and CD163 (red) to analyze macrophage polarization by visualizing $F4/80^+CD163^-$ M1 macrophages and $F4/80^+CD163^+$ M2 macrophages. Scale bar indicates 100 μm. Quantification of (E) total macrophages ($F4/80^+$ cells) in ischemic muscle ($n = 13–15$; $^{**}p < .01$ versus PBS, HDL, and SP groups, $+p < .05$ versus normal group) and (F) the ratio of M2 type macrophages ($F4/80^+/CD163^+$ cells) to total macrophages ($F4/80^+$ cells) ($n = 13–15$; $^{**}p < .01$ versus other groups, $++p < .01$ versus PBS group, and $\#p < .05$ versus SP group). (For interpretation of the references to color in this figure legend, the reader is referred to the Web version of this article.)

modulating effect even better than SP administration (40.1 ± 6.1% in HDL group and 29.1 ± 5.4% in SP group, Fig. 4F). Previous studies demonstrated that HDL binds to the toll-like receptor of pro-inflammatory macrophages and gives negative feedback by changing intracellular signaling [41]. Subsequently, the macrophages activated by HDL were found to express M2 phenotypic genes [42]. As a result, HDL itself could also show immune modulating effect for tissue healing by inducing anti-inflammatory responses in the injured muscles.

HDL-SP nanodiscs could significantly reduce serious physiological complications such as splenomegaly, a hypertrophy of spleen, caused by severe inflammatory responses after tissue injury [6,43]. The size of spleen was increased by diabetic ischemic injury (Fig. 5A). When compared to PBS injection, HDL or SP treatment did not prevent the increase in the weight ratio of spleen (13.8 ± 2.1 g kg^{-1} mouse for PBS group, 12.1 ± 3.5 g kg^{-1} mouse for HDL group, and 12.9 ± 2.9 g kg^{-1} mouse for SP group, Fig. 5B). The attenuation of inflammatory responses in diabetic mice with hindlimb ischemia by HDL-SP administration contributed to inhibition of the increase in the size and weight of spleen (9.0 ± 1.7 g kg^{-1} mouse for HDL-SP group, Fig. 5A and B). In the spleen, there are two different areas; red blood cell (RBC)-rich red pulp and immune cell-rich white pulp. The area of white pulp indicates the inflammation [44]. Five days after ischemia induction and injection treatments in

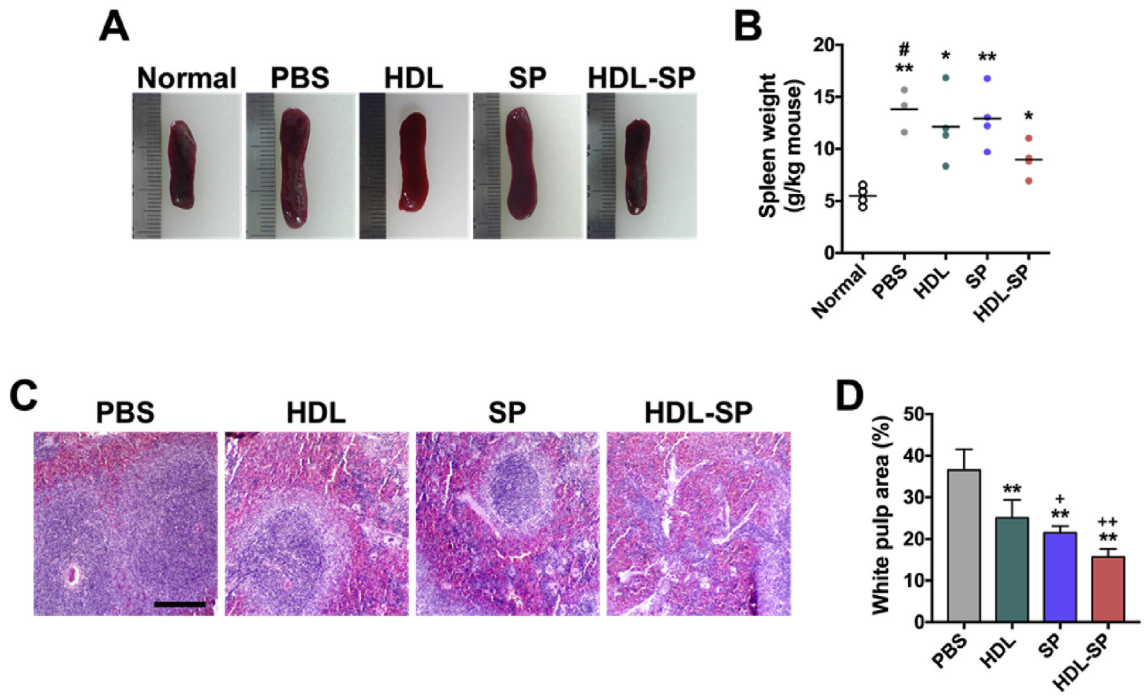

Fig. 5. Attenuation of inflammation-associated spleen enlargement by HDL-SP administration in a diabetic hindlimb ischemia model. (A) Representative images of spleens 5 days after ischemia induction and injection treatments. (B) Spleen weights normalized to body weight of each mouse ($n = 4$; $^{*}p < .05$ and $^{**}p < .01$ versus normal group, $\#p < .05$ versus HDL-SP group). (C) H&E staining of cross-sectioned spleen. Immune cell-rich area (blue-colored region) in each image indicates white pulp. Scale bar indicates 1 mm. (D) Quantification of white pulp area in total spleen ($n = 4$; $^{**}p < .01$ versus PBS group, $+p < .05$ and $++p < .01$ versus HDL group). (For interpretation of the references to color in this figure legend, the reader is referred to the Web version of this article.)

diabetic mice (2.5 nmol kg^{-1} of SP and HDL-SP), the ratio of white pulp area within total area of spleen was significantly decreased in HDL-SP group ($15.7 \pm 2.0\%$ for HDL-SP group), compared to other groups ($36.5 \pm 5.0\%$ for PBS group, $25.1 \pm 4.3\%$ for HDL group, and $21.5 \pm 1.6\%$ for SP group, Fig. 5C and D). Overall, HDL-SP nanodisc formulation potentiated immune modulation of SP treatment, which prevents inflammation-associated second tissue damage and facilitates wound healing process in diabetic hindlimb ischemia.

3.5. Improved ischemic limb salvage and blood perfusion restoration by HDL-SP nanodiscs in diabetic hindlimb ischemia

In a diabetic hindlimb ischemia induced by femoral artery ligation and excision, injection treatment of HDL-SP nanodiscs exhibited enhanced therapeutic efficacy by effectively prompting blood perfusion recovery and improving ischemic limb salvage probably due to the extended circulatory half-life, facilitated stem cell mobilization, and potentiated immune-regulatory function by HDL modification. To evaluate the therapeutic effects of HDL-SP on ischemic limb salvage and blood perfusion restoration, the physiological score of ischemic limb status and the recovery of blood flow in ischemic limb were analyzed 4 week-post ischemia induction and treatments. The protocol for diabetes induction, ischemic injury, and injection regimens is shown in Fig. 6A. After 28 days of injection, HDL-SP treatment led to significant reduction of ischemic limb loss or necrosis and much greater salvage of the ischemic limb (76.9%), compared to PBS (15.4%), HDL (35.7%), SP (21.4%), and LIPO-SP treatments (14.3%) (Fig. 6B and C). Interestingly, HDL administration showed improved ischemic limb salvage and reduced limb amputation, compared to unmodified SP treatment (35.7% limb loss, 35.7% limb salvage for HDL group versus 57.1% limb loss, 21.4% limb salvage for SP group, Fig. 6C). This might be because under diabetic conditions the endogenous stem cell mobilizing effect of SP is significantly attenuated by increased NEP activity and the immune modulating effect of HDL is greater than SP (Figs. 3–5). Despite reduced limb amputation by HDL treatment in comparison to SP treatment, more than 60% of the mice still underwent ischemic limb loss and necrosis (Fig. 6C). Thus, the synergistic effect of stem cell mobilization and immune modulation of HDL-SP nanodiscs would be of great importance for therapeutic angiogenesis in diabetic peripheral ischemia. The significant improvement in blood perfusion in diabetic ischemic muscle could be achieved by injection treatment of HDL-SP nanodiscs. Laser Doppler flowmeter analysis quantifying the recovery of blood flow revealed that HDL-SP group showed the most improved blood perfusion restoration, compared to control groups (PBS, HDL, SP, and LIPO-SP) at all-time points for the analysis (Fig. 6D and E). The rapid restoration of blood flow by HDL-SP therapy in the early stage of ischemia progress effectively prevented limb necrosis or loss and consequently improved ischemic limb salvage.

3.6. Promoted blood vessel formation and prevention of muscle degeneration and fibrosis by HDL-SP nanodiscs in a diabetic hindlimb ischemia

HDL-SP treatment effectively prevented muscle degeneration and fibrosis in diabetic ischemic muscle. Histological analyses of hematoxylin & eosin (H&E) and Masson's trichrome staining with ischemic muscle 28 days after treatment revealed that muscle degeneration, abnormal muscle structures, and the infiltration of adipocytes were observed in control treatment groups (PBS, HDL, SP, and LIPO-SP), whereas muscle degeneration was significantly attenuated in HDL-SP treatment group (Fig. 7A). The fibrosis in ischemic muscle was also significantly reduced in HDL-SP group, compared with that in control groups (PBS, HDL, SP, and LIPO-SP,

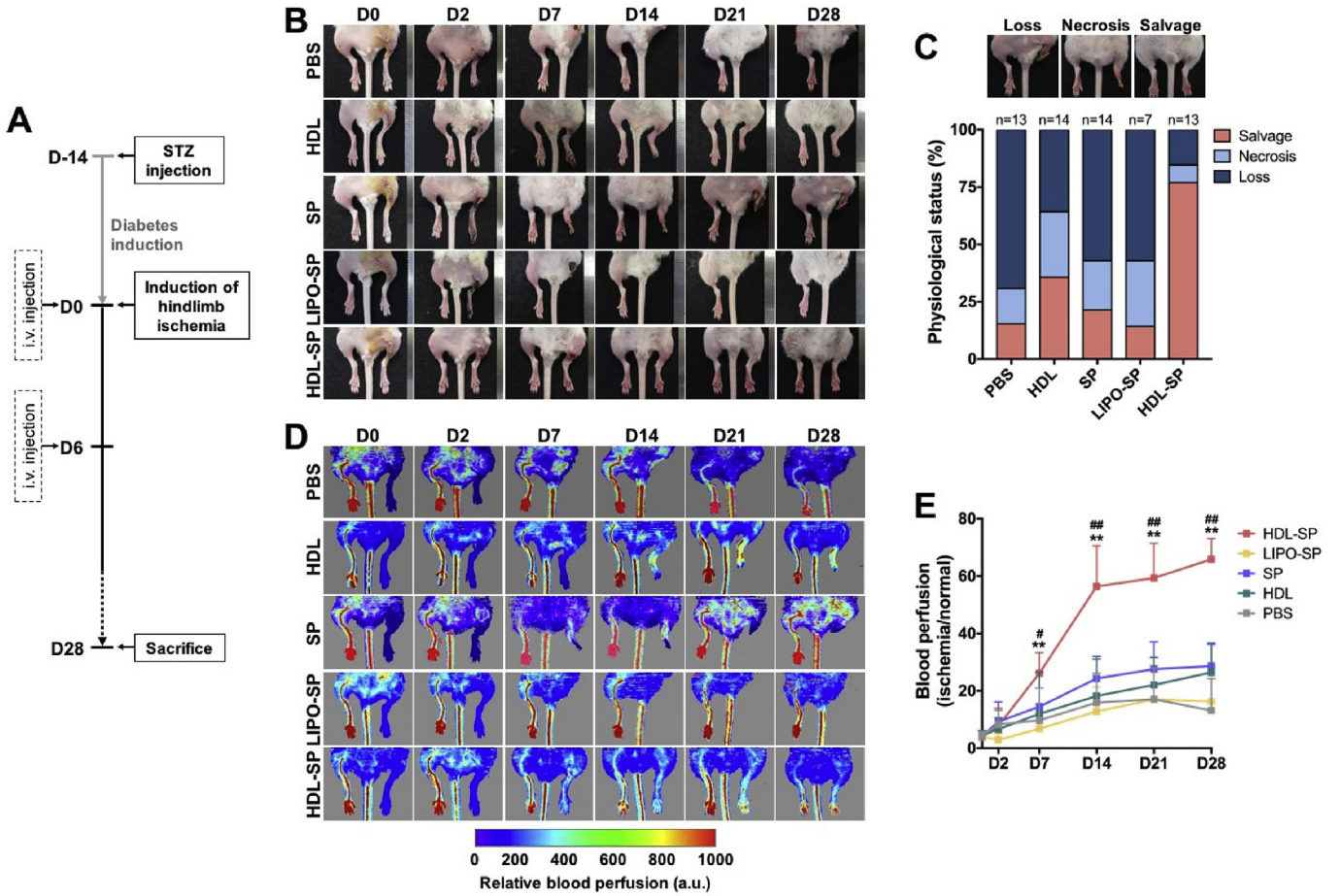

Fig. 6. Improved ischemic limb salvage by HDL-SP administration in a diabetic hindlimb ischemia model. (A) Experimental scheme showing the time-line of diabetes and ischemia induction, injection treatments, and sample analyses. (B) Representative images of diabetic ischemic limbs of each group. (C) Scoring of physiological status of diabetic ischemic limb 28 days after ischemic injury and injection treatments ($n = 7–14$). (D) Serial analyses of blood reperfusion in ischemic limb using Doppler Flowmeter. (E) Quantification of blood reperfusion by calculating the perfusion ratio of ischemic limb to normal limb on days 0, 2, 7, 14, 21, and 28 after ischemic injury and injection treatments ($n = 6$; $^{**}p < .01$ versus PBS, HDL, and LIPO-SP groups, $\#p < .05$ and $\#\#p < .01$ versus SP group).

Fig. 7B, E). The vascular density was remarkably increased in ischemic muscle treated with HDL-SP nanodiscs, as confirmed by immunohistochemical staining of the CD31-positive capillary and SMA-positive arteriole (Fig. 7C and D). The densities of the CD31-positive capillary and SMA-positive arteriole were the highest in HDL-SP-treated ischemic muscle (Fig. 7F and G). The average size of the arterioles was the largest in the HDL-SP group compared to other groups, indicating that HDL-SP facilitated blood vessel formation and vascular maturation in ischemic muscle ($109 \pm 75\ mm^2$ in PBS group, $187 \pm 111\ mm^2$ in HDL group, $200 \pm 98\ mm^2$ in SP group, $294 \pm 211\ mm^2$ in LIPO-SP group, and $505 \pm 257\ mm^2$ in HDL-SP group, Fig. 7H). These results demonstrate that HDL-SP with increased circulating half-life and bone marrow retention can significantly improve therapeutic angiogenesis for the treatment of diabetic peripheral ischemia.

Our strategy using HDL-mimicking nanodisc formulation for systemic delivery of therapeutic peptides would provide some advantages over conventional methods for delivery and bone marrow targeting of proteins and peptides. Many nanotechnology-based delivery systems for therapeutic proteins and peptides have been developed utilizing liposomes, dendrimers, and polymer nanoparticles to increase therapeutic effectiveness of polypeptides by targeting to specific organ/tissue and protecting from degradation by serum protease [10,14,15,45,46]. However, those approaches still have limitations such as low delivery efficiency, loss of drug activity, unwanted binding to circulating blood cells, and cytotoxicity [47,48]. Several chemical or physical modification methods of proteins and peptides have also been tested to enhance their therapeutic efficacy by increasing *in vivo* half-life of administered drugs [49]. For example, polyethylene glycol (PEG) conjugation, commonly termed as PEGylation, to proteins and peptides has been one of the most widely used modification strategies to solve limited efficacy due to short half-life of peptide and protein drugs [12,49]. However, in some instances, PEGylation causes conformational change in molecular structures of proteins/peptides or shields their receptor-binding sites, leading to inhibition of binding to target receptors, and resulting in decreased activity and low therapeutic effect [49,50]. In contrast to these conventional approaches, our HDL-based nanoparticle formulation could circumvent these critical issues by harboring only MPB portion conjugated to SP into HDL nanodiscs and leaving a receptor binding site of SP (C-terminus) available for binding to NK1R (Fig. 1A and B) [24,25]. Due to the presence of the amphipathic core lipoprotein, HDL-SP nanodiscs become water-soluble and can thus be transported through blood and lymph. In addition, HDL-SP nanodiscs in the context of natural HDL-mimicking nanoparticles could effectively protect SP from NEP-mediated degradation in blood circulation, resulting in significant extension of *in vivo* half-life up to 1060 folds compared to unmodified SP peptides after systemic administration (Fig. 2C). Therefore, HDL-based nanodisc formulation could offer a promising

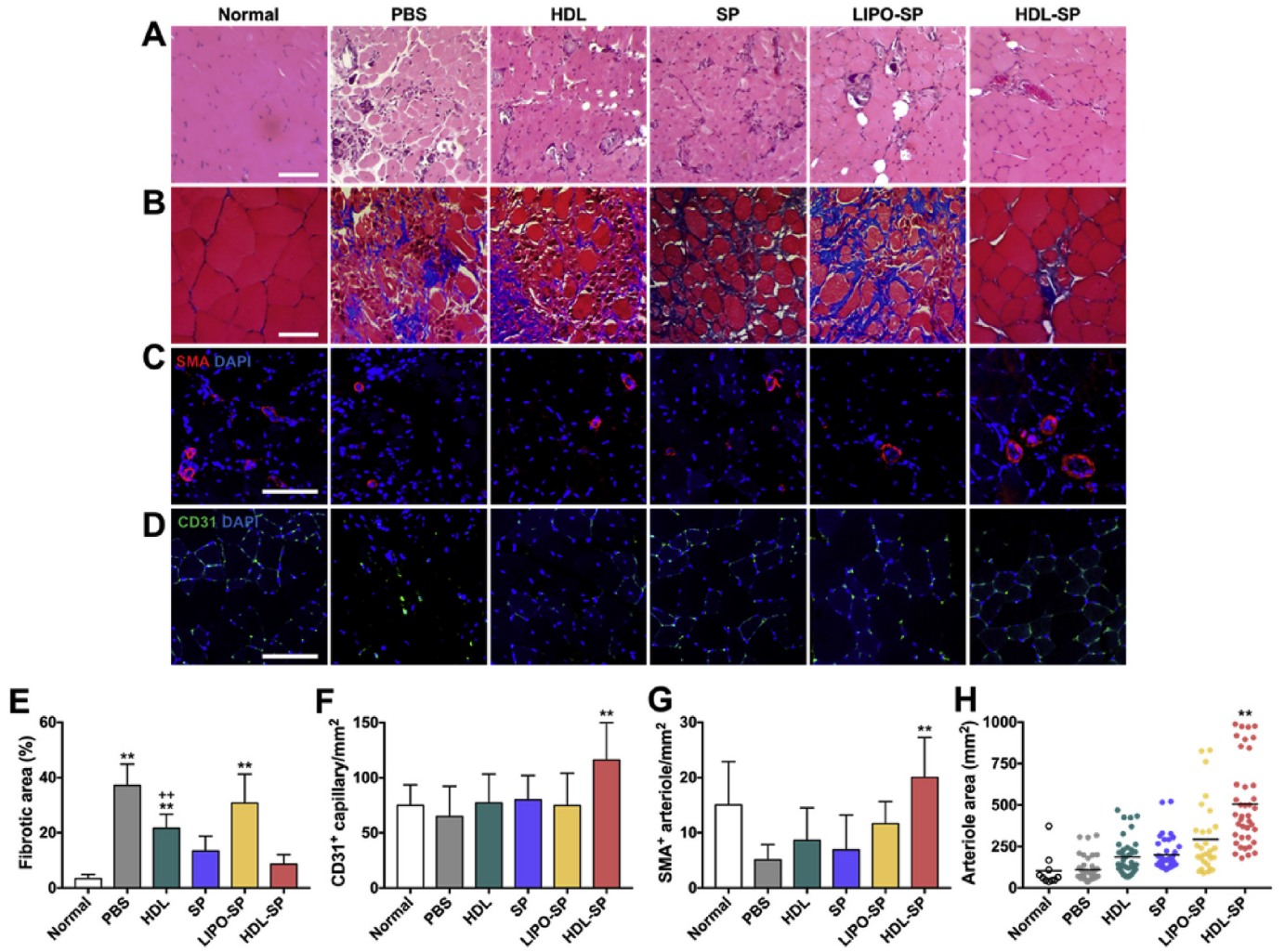

Fig. 7. Improved therapeutic angiogenesis 28 days after HDL-SP administration to a mouse model of diabetic hindlimb ischemia. (A) H&E and (B) Masson's trichrome staining 28 days after ischemic injury and injection treatments. Scale bars indicate 100 μm. Immunofluorescent staining of (C) SMA-positive arterioles and (D) CD31-positive capillaries in ischemic muscle 28 days after ischemic injury and injection treatments. Scale bars indicate 100 μm. (E) Fibrotic area in ischemic region quantified from Masson's trichrome-stained images ($n = 15$; $^{**}p < .01$ versus HDL-SP group, $++p < .01$ versus SP group). The density of (F) CD31-positive capillaries and (G) SMA-positive arterioles in ischemic muscle ($n = 10–30$; $^{**}p < .01$ versus other groups). (H) The average area of SMA-positive arterioles in ischemic region ($n = 10–20$; $^{**}p < .01$ versus other groups).

and versatile bio-mimetic strategy to substantially improve the efficacy of therapeutic peptides.

4. Conclusions

In summary, we report a bio-inspired modification to potentiate therapeutic efficacy of a peptide drug by inducing synergistic effect of endogenous stem cell mobilization and immune modulation for diabetic hindlimb ischemia treatment. The HDL-mimicking nanodisc formulation of SP peptide, an endogenous stem cell mobilizer, remarkably extended the circulatory half-life of SP *in vivo* and retention time in bone marrow, a target organ for SP function, with no detectable hepatotoxicity. The improved pharmacokinetic properties of HDL-SP nanodisc formulation not only boosted mobilization of endogenous bone marrow stem/progenitor cells (MSCs and EPCs), but also potentiated immune modulating effects of SP by suppressing pro-inflammatory cytokine (TNF-α) secretion, increasing anti-inflammatory cytokine (IL-10) secretion, and activating M2-phase polarization of infiltrated macrophages. Ultimately, HDL-SP nanodiscs could enhance the therapeutic and regenerative capacity of SP therapy by increasing blood vessel formation and inhibiting muscle degeneration/fibrosis in diabetic hindlimb ischemia, leading to improved ischemic limb salvage and decreased limb loss/necrosis. Therefore, HDL-SP enables highly effective stem cell-free therapy for the treatment of diabetic peripheral ischemia. HDL-SP nanodiscs would also be applicable for other diabetic complications such as diabetic ulcer, cardiomyopathy, and retinopathy. The use of HDL-mimicking nanodisc formulations would be further expanded to modification and functionalization of other peptide or protein drugs in regenerative medicine.

Acknowledgements

This work was supported by a grant (H13C1479) from the Korea Health Technology R&D Project funded by the Ministry of Health, and Welfare, a grant (2017R1A2B3005994) from the National Research Foundation of Korea (NRF), a grant (IBS-R026-D1) from the Institute for Basic Science (IBS), Republic of Korea, and a grant (R01HL134569) from National Institutes of Health (NIH). Dr. Hyun-Ji Park was partially supported by the Yonsei University Research Fund (Post-Doc. Researcher Supporting Program of 2017; Project No. 2017-12-0200). We acknowledge Dr. Dhabaleswar Patra and Prof. Georgios Skiniotis for help with TEM imaging. Rui Kuai was

partially supported by the Broomfield International Student Fellowship and the AHA Predoctoral Fellowship (15PRE25090050).

Appendix A. Supplementary data

Supplementary data related to this article can be found at https://doi.org/10.1016/j.biomaterials.2018.01.027.

References

[1] C.A. Herberts, M.S. Kwa, H.P. Hermsen, Risk factors in the development of stem cell therapy, J. Transl. Med. 9 (2011) 29.
[2] I.K. Ko, S.J. Lee, A. Atala, J.J. Yoo, In situ tissue regeneration through host stem cell recruitment, Exp. Mol. Med. 45 (2013) e57.
[3] F.D. Miller, D.R. Kaplan, Mobilizing endogenous stem cells for repair and regeneration: are we there yet? Cell Stem Cell 10 (6) (2012) 650–652.
[4] H.S. Hong, J. Lee, E. Lee, Y.S. Kwon, E. Lee, W. Ahn, M.H. Jiang, J.C. Kim, Y. Son, A new role of substance P as an injury-inducible messenger for mobilization of CD29(+) stromal-like cells, Nat. Med. 15 (4) (2009) 425–435.
[5] S. Amadesi, C. Reni, R. Katare, M. Meloni, A. Oikawa, A.P. Beltrami, E. Avolio, D. Cesselli, O. Fortunato, G. Spinetti, R. Ascione, E. Cangiano, M. Valgimigli, S.P. Hunt, C. Emanueli, P. Madeddu, Role for substance P-based nociceptive signaling in progenitor cell activation and angiogenesis during ischemia in mice and in human subjects, Circulation 125 (14) (2012) 1774–1786.
[6] J.H. Park, S. Kim, H.S. Hong, Y. Son, Substance P promotes diabetic wound healing by modulating inflammation and restoring cellular activity of mesenchymal stem cells, Wound Repair Regen. 24 (2) (2016) 337–348.
[7] H.S. Hong, S. Kim, S. Nam, J. Um, Y.H. Kim, Y. Son, Effect of substance P on recovery from laser-induced retinal degeneration, Wound Repair Regen. 23 (2) (2015) 268–277.
[8] M.H. Jiang, J.E. Lim, G.F. Chi, W. Ahn, M. Zhang, E. Chung, Y. Son, Substance P reduces apoptotic cell death possibly by modulating the immune response at the early stage after spinal cord injury, Neuroreport 24 (15) (2013) 846–851.
[9] S. Mitragotri, P.A. Burke, R. Langer, Overcoming the challenges in administering biopharmaceuticals: formulation and delivery strategies, Nat. Rev. Drug Discov. 13 (9) (2014) 655–672.
[10] P. Muangman, M.L. Spenny, R.N. Tamura, N.S. Gibran, Fatty acids and glucose increase neutral endopeptidase activity in human microvascular endothelial cells, Shock 19 (6) (2003) 508–512.
[11] J.J. Bowden, A.M. Garland, P. Baluk, P. Lefevre, E.F. Grady, S.R. Vigna, N.W. Bunnett, D.M. McDonald, Direct observation of substance P-induced internalization of Neurokinin 1 (NK1) receptors at sites of inflammation, Proc. Natl. Acad. Sci. U. S. A 91 (19) (1994) 8964–8968.
[12] M.J. Roberts, M.D. Bentley, J.M. Harris, Chemistry for peptide and protein PEGylation, Adv. Drug Deliv. Rev. 54 (4) (2002) 459–476.
[13] A.J. Garber, Will the next generation of basal insulins offer clinical advantages? Diabetes Obes. Metabol. 16 (6) (2014) 483–491.
[14] D. Sleep, J. Cameron, L.R. Evans, Albumin as a versatile platform for drug half-life extension, Biochim. Biophys. Acta 1830 (12) (2013) 5526–5534.
[15] R.E. Kontermann, Strategies for extended serum half-life of protein therapeutics, Curr. Opin. Biotechnol. 22 (6) (2011) 868–876.
[16] R. Kuai, D. Li, Y.E. Chen, J.J. Moon, A. Schwendeman, High-density lipoproteins: nature's multifunctional nanoparticles, ACS Nano 10 (3) (2016) 3015–3041.
[17] B.L. Trigatti, M. Krieger, A. Rigotti, Influence of the HDL receptor SR-BI on lipoprotein metabolism and atherosclerosis, Arterioscler. Thromb. Vasc. Biol. 23 (10) (2003) 1732–1738.
[18] M. Hoekstra, SR-BI as target in atherosclerosis and cardiovascular disease - a comprehensive appraisal of the cellular functions of SR-BI in physiology and disease, Atherosclerosis 258 (2017) 153–161.
[19] R. Kuai, L.J. Ochyl, K.S. Bahjat, A. Schwendeman, J.J. Moon, Designer vaccine nanodiscs for personalized cancer immunotherapy, Nat. Mater. 16 (4) (2017) 489–496.
[20] L. Camont, M. Lhomme, F. Rached, W. Le Goff, A. Negre-Salvayre, R. Salvayre, C. Calzada, M. Lagarde, M.J. Chapman, A. Kontush, Small, dense high-density Lipoprotein-3 particles are enriched in negatively charged phospholipids: relevance to cellular cholesterol efflux, antioxidative, antithrombotic, anti-inflammatory, and antiapoptotic functionalities, Arterioscler. Thromb. Vasc. Biol. 33 (12) (2013) 2715–2723.
[21] M.M.K. Shahzad, L.S. Mangala, H.D. Han, C. Lu, J. Bottsford-Miller, M. Nishimura, E.M. Mora, J.-W. Lee, R.L. Stone, C.V. Pecot, D. Thanapprapasr, J.-W. Roh, P. Gaur, M.P. Nair, Y.-Y. Park, N. Sabnis, M.T. Deavers, J.-S. Lee, L.M. Ellis, G. Lopez-Berestein, W.J. McConathy, L. Prokai, A.G. Lacko, A.K. Sood, Targeted delivery of small interfering RNA using reconstituted high-density lipoprotein nanoparticles, Neoplasia 13 (4) (2011) 309–319.
[22] H.J. Park, Y. Jin, J. Shin, K. Yang, C. Lee, H.S. Yang, S.W. Cho, Catechol-functionalized hyaluronic acid hydrogels enhance angiogenesis and osteogenesis of human adipose-derived stem cells in critical tissue defects, Biomacromolecules 17 (6) (2016) 1939–1948.
[23] J. Lee, I. Jun, H.J. Park, T.J. Kang, H. Shin, S.W. Cho, Genetically engineered myoblast sheet for therapeutic angiogenesis, Biomacromolecules 15 (1) (2014) 361–372.
[24] M.S. Steinhoff, B. von Mentzer, P. Geppetti, C. Pothoulakis, N.W. Bunnett, Tachykinins and their receptors: contributions to physiological control and the mechanisms of disease, Physiol. Rev. 94 (1) (2014) 265–301.
[25] L. Valentin-Hansen, M. Park, T. Huber, A. Grunbeck, S. Naganathan, T.W. Schwartz, T.P. Sakmar, Mapping substance P binding sites on the Neurokinin-1 receptor using genetic incorporation of a photoreactive amino acid, J. Biol. Chem. 289 (26) (2014) 18045–18054.
[26] Y. Zhao, T. Imura, L.J. Leman, L.K. Curtiss, B.E. Maryanoff, M.R. Ghadiri, Mimicry of high-density lipoprotein: functional peptide-lipid nanoparticles based on multivalent peptide constructs, J. Am. Chem. Soc. 135 (36) (2013) 13414–13424.
[27] J. Wu, R. Zou, Q. Wang, Y. Xue, P. Wei, S. Yang, J. Wu, H. Tian, A peptide probe for the detection of neurokinin-1 receptor by disaggregation enhanced fluorescence and magnetic resonance signals, Sci. Rep. 4 (2014) 6487.
[28] F. Rezaee, B. Casetta, J.H. Levels, D. Speijer, J.C. Meijers, Proteomic analysis of high-density lipoprotein, Proteomics 6 (2) (2006) 721–730.
[29] E. Eren, N. Yilmaz, O. Aydin, High density lipoprotein and it's dysfunction, Open Biochem. J. 6 (2012) 78–93.
[30] B.J. Bruno, G.D. Miller, C.S. Lim, Basics and recent advances in peptide and protein drug delivery, Ther. Deliv. 4 (11) (2013) 1443–1467.
[31] H.K. Yu, H.J. Lee, J.H. Ahn, I.H. Lim, J.H. Moon, Y. Yoon, L.S. Yi, S.J. Kim, J.S. Kim, Immunoglobulin Fc domain fusion to apolipoprotein(a) kringle V significantly prolongs plasma half-life without affecting its anti-angiogenic activity, Protein Eng. Des. Sel. 26 (6) (2013) 425–432.
[32] A. Zorzi, S.J. Middendorp, J. Wilbs, K. Deyle, C. Heinis, Acylated heptapeptide binds albumin with high affinity and application as tag furnishes long-acting peptides, Nat. Commun. 8 (2017) 16092.
[33] L.H. Huang, A. Elvington, G.J. Randolph, The role of the lymphatic system in cholesterol transport, Front. Pharmacol. 6 (2015) 182.
[34] S.D. Covey, M. Krieger, W. Wang, M. Penman, B.L. Trigatti, Scavenger receptor class B type I-mediated protection against atherosclerosis in LDL receptor-negative mice involves its expression in bone marrow-derived cells, Arterioscler. Thromb. Vasc. Biol. 23 (9) (2003) 1589–1594.
[35] M. Gao, D. Zhao, S. Schouteden, M.G. Sorci-Thomas, P.P. Van Veldhoven, K. Eggermont, G. Liu, C.M. Verfaillie, Y. Feng, Regulation of high-density lipoprotein on hematopoietic stem/progenitor cells in atherosclerosis requires scavenger receptor type BI expression, Arterioscler. Thromb. Vasc. Biol. 34 (9) (2014) 1900–1909.
[36] R.C. Rennert, M. Sorkin, M. Januszyk, D. Duscher, R. Kosaraju, M.T. Chung, J. Lennon, A. Radiya-Dixit, S. Raghvendra, Z.N. Maan, M.S. Hu, J. Rajadas, M. Rodrigues, G.C. Gurtner, Diabetes impairs the angiogenic potential of adipose-derived stem cells by selectively depleting cellular subpopulations, Stem Cell Res. Ther. 5 (3) (2014) 79.
[37] Y. Jin, H.S. Hong, Y. Son, Substance P enhances mesenchymal stem cells-mediated immune modulation, Cytokine 71 (2) (2015) 145–153.
[38] M.Y. Donath, S.E. Shoelson, Type 2 diabetes as an inflammatory disease, Nat. Rev. Immunol. 11 (2) (2011) 98–107.
[39] M.H. Jiang, E. Chung, G.F. Chi, W. Ahn, J.E. Lim, H.S. Hong, D.W. Kim, H. Choi, J. Kim, Y. Son, Substance P induces M2-type macrophages after spinal cord injury, Neuroreport 23 (13) (2012) 786–792.
[40] A. Sica, A. Mantovani, Macrophage plasticity and polarization: in vivo veritas, J. Clin. Invest. 122 (3) (2012) 787–795.
[41] D. De Nardo, L.I. Labzin, H. Kono, R. Seki, S.V. Schmidt, M. Beyer, D. Xu, S. Zimmer, C. Lahrmann, F.A. Schildberg, J. Vogelhuber, M. Kraut, T. Ulas, A. Kerksiek, W. Krebs, N. Bode, A. Grebe, M.L. Fitzgerald, N.J. Hernandez, B.R. Williams, P. Knolle, M. Kneilling, M. Rocken, D. Lutjohann, S.D. Wright, J.L. Schultze, E. Latz, High-density lipoprotein mediates anti-inflammatory reprogramming of macrophages via the transcriptional regulator ATF3, Nat. Immunol. 15 (2) (2014) 152–160.
[42] M. Sanson, E. Distel, E.A. Fisher, HDL induces the expression of the M2 macrophage markers Arginase 1 and Fizz-1 in a STAT6-dependent process, PLoS One 8 (8) (2013), e74676.
[43] E. Tolosano, S. Fagoonee, E. Hirsch, F.G. Berger, H. Baumann, L. Silengo, F. Altruda, Enhanced splenomegaly and severe liver inflammation in haptoglobin/hemopexin double-null mice after acute hemolysis, Blood 100 (12) (2002) 4201–4208.
[44] J.G. Kiang, M. Zhai, P.J. Liao, D.L. Bolduc, T.B. Elliott, N.V. Gorbunov, Pegylated G-CSF inhibits blood cell depletion, increases platelets, blocks splenomegaly, and improves survival after whole-body ionizing irradiation but not after irradiation combined with burn, Oxid. Med. Cell. Longev 2014 (2014), 481392.
[45] Z.Y. Jiang, S.W. Xu, Y.Q. Wang, Chemistry for pegylation of protein and peptide molecules, Chin. J. Org. Chem. 23 (12) (2003) 1340–1347.
[46] V.P. Torchilin, Multifunctional, stimuli-sensitive nanoparticulate systems for drug delivery, Nat. Rev. Drug Discov. 13 (11) (2014) 813–827.
[47] H. Chang, J. Lv, X. Gao, X. Wang, H. Wang, H. Chen, X. He, L. Li, Y. Cheng, Rational design of a polymer with robust efficacy for intracellular protein and peptide delivery, Nano Lett. 17 (3) (2017) 1678–1684.
[48] N. Matougui, L. Boge, A.C. Groo, A. Umerska, L. Ringstad, H. Bysell, P. Saulnier, Lipid-based nanoformulations for peptide delivery, Int. J. Pharm. 502 (1–2) (2016) 80–97.
[49] J.M. Harris, R.B. Chess, Effect of pegylation on pharmaceuticals, Nat. Rev. Drug Discov. 2 (3) (2003) 214–221.
[50] J.M. Harris, N.E. Martin, M. Modi, Pegylation: a novel process for modifying pharmacokinetics, Clin. Pharmacokinet 40 (7) (2001) 539–551.